Whole-exome sequencing reveals novel cancer genes and actionable targets in biliary tract cancers in primary sclerosing cholangitis

VISUAL ABSTRACT

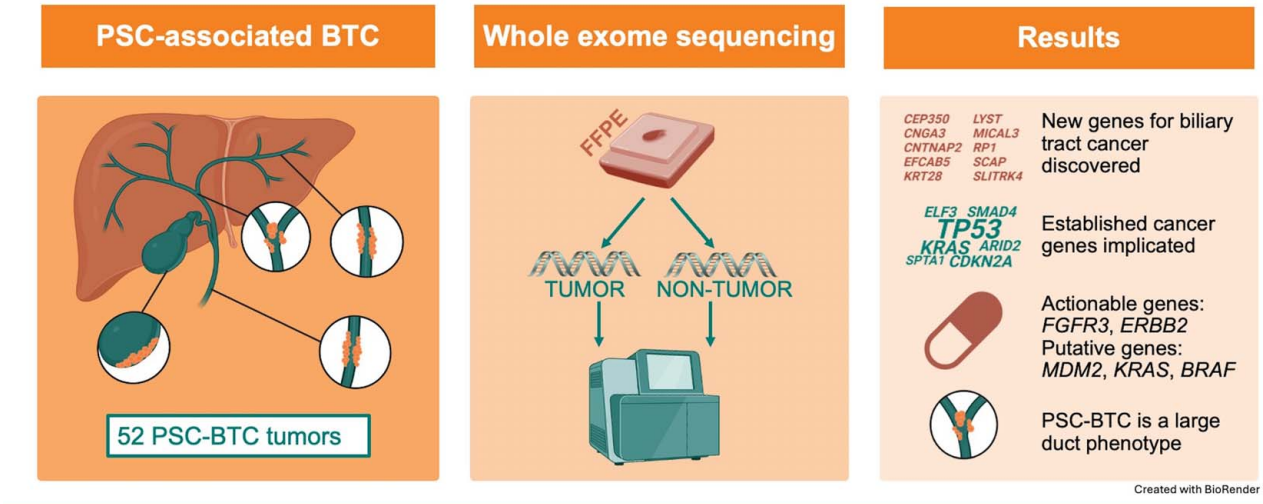

Received: 29 September 2023 | Accepted: 13 March 2024

DOI: 10.1097/HC9.0000000000000461

ORIGINAL ARTICLE

OPEN

Whole-exome sequencing reveals novel cancer genes and actionable targets in biliary tract cancers in primary sclerosing cholangitis

Marit M. Grimsrud[1,2,3] | Michael Forster[4] | Benjamin Goeppert[5,6,7] | Georg Hemmrich-Stanisak[4] | Irmi Sax[8] | Krzysztof Grzyb[9] | Peder R. Braadland[1,2,3] | Alphonse Charbel[5] | Carmen Metzger[5] | Thomas Albrecht[5] | Tim Alexander Steiert[4] | Matthias Schlesner[8] | Michael P. Manns[10] | Arndt Vogel[10] | Sheraz Yaqub[2,11] | Tom H. Karlsen[1,2,3,12] | Peter Schirmacher[5] | Kirsten M. Boberg[1,2,3,12] | Andre Franke[4] | Stephanie Roessler[5] | Trine Folseraas[1,2,3,12]

[1]Department of Transplantation Medicine, Division of Surgery, Inflammatory Medicine and Transplantation, Norwegian PSC Research Center, Oslo University Hospital Rikshospitalet, Oslo, Norway

[2]Institute of Clinical Medicine, Faculty of Medicine, University of Oslo, Oslo, Norway

[3]Research Institute of Internal Medicine, Division of Surgery, Inflammatory Medicine and Transplantation, Oslo University Hospital Rikshospitalet, Oslo, Norway

[4]Institute of Clinical Molecular Biology, Christian-Albrechts-University, Kiel, Germany

[5]Institute of Pathology, University Hospital Heidelberg, Heidelberg University, Heidelberg, Germany

[6]Institute of Pathology, Hospital RKH Kliniken Ludwigsburg, Ludwigsburg, Germany

[7]Institute of Tissue Medicine and Pathology, University of Bern, Bern, Switzerland

[8]Biomedical Informatics, Data Mining and Data Analytics, University of Augsburg, Augsburg, Germany

[9]Department of Pathology, Oslo University Hospital, Oslo, Norway

[10]Department of Gastroenterology, Hepatology and Endocrinology, Hannover Medical School, Hannover, Germany

[11]Department of Hepatobiliary Surgery, Oslo University Hospital, Oslo, Norway

[12]Section for Gastroenterology, Department of Transplantation Medicine, Division of Surgery, Inflammatory Medicine and Transplantation, Oslo University Hospital Rikshospitalet, Oslo, Norway

Correspondence
Trine Folseraas, Department of Transplantation Medicine, Division of Surgery, Inflammatory Medicine and Transplantation, Oslo University Hospital Rikshospitalet, Postboks 4950 Nydalen, Oslo N-0424, Norway.
Email: trine.folseraas@medisin.uio.no

Abstract

Background: People with primary sclerosing cholangitis (PSC) have a 20% lifetime risk of biliary tract cancer (BTC). Using whole-exome sequencing, we characterized genomic alterations in tissue samples from BTC with underlying PSC.

Abbreviations: AF, allele frequency; AJCC, American Joint Committee on Cancer classification; BTC, biliary tract cancer; CCA, cholangiocarcinoma; CISH, chromogen-in-situ-hybridization; CNV, copy number variation; FFPE, formalin-fixed paraffin-embedded; iCCA, intrahepatic cholangiocarcinoma; IHC, immunohistochemistry; NOS, not otherwise specified; PSC, primary sclerosing cholangitis; PSC-BTC, primary sclerosing cholangitis-associated biliary tract cancer; TMA, tissue microarray.

Marit M. Grimsrud and Michael Forster contributed equally to this work and therefore share the first authorship.

Stephanie Roessler and Trine Folseraas contributed equally to this work and therefore share the last authorship.

Supplemental Digital Content is available for this article. Direct URL citations are provided in the HTML and PDF versions of this article on the journal's website, www.hepcommjournal.com.

Methods: We extracted DNA from formalin-fixed, paraffin-embedded tumor and paired nontumor tissue from 52 resection or biopsy specimens from patients with PSC and BTC and performed whole-exome sequencing. Following copy number analysis, variant calling, and filtering, putative PSC-BTC-associated genes were assessed by pathway analyses and annotated to targeted cancer therapies.

Results: We identified 53 candidate cancer genes with a total of 123 nonsynonymous alterations passing filtering thresholds in 2 or more samples. Of the identified genes, 19% had not previously been implicated in BTC, including *CNGA3, KRT28*, and *EFCAB5*. Another subset comprised genes previously implicated in hepato-pancreato-biliary cancer, such as *ARID2, ELF3*, and *PTPRD.* Finally, we identified a subset of genes implicated in a wide range of cancers such as the tumor suppressor genes *TP53*, *CDKN2A*, *SMAD4*, and *RNF43* and the oncogenes *KRAS*, *ERBB2*, and *BRAF*. Focal copy number variations were found in 51.9% of the samples. Alterations in potential actionable genes, including *ERBB2*, *MDM2*, and *FGFR3* were identified and alterations in the RTK/RAS ($p = 0.036$), TP53 ($p = 0.04$), and PI3K ($p = 0.043$) pathways were significantly associated with reduced overall survival.

Conclusions: In this exome-wide characterization of PSC-associated BTC, we delineated both PSC-specific and universal cancer genes. Our findings provide opportunities for a better understanding of the development of BTC in PSC and could be used as a platform to develop personalized treatment approaches.

INTRODUCTION

The immune-mediated bile duct disease, primary sclerosing cholangitis (PSC), is an important risk factor for biliary tract cancer (BTC).[1] BTC, encompassing cholangiocarcinoma (CCA) and gallbladder carcinoma, affects up to 20% of people with PSC and may occur at any disease stage.[1,2] Liver transplantation is an effective curative treatment for PSC, but BTC development normally contraindicates liver transplantation and is currently responsible for up to half of the PSC-associated mortality.[2,3] The prognosis of PSC-associated BTC (PSC-BTC) remains poor due to ineffective early detection strategies and limited treatment options.[4]

BTC in patients with PSC is likely to result from chronic biliary inflammation, cholestasis, and recurrent biliary infections.[3] Bile acid toxicity, oxidative stress, and activation of EGFR, COX-2, and KRas pathways are believed to drive neoplastic proliferation and genomic instability.[5] Multiple lines of evidence point to a gradual malignant transformation of the biliary epithelium in PSC, where preneoplastic biliary intraepithelial and intraductal papillary neoplasms precede invasive BTC.[6] Only a few low-risk germline genetic variants have been found to increase the risk of BTC in people with PSC, suggesting that inheritance plays a minor role in the etiology.[4,6]

Previous targeted sequencing studies of known somatic tumor suppressor genes and oncogenes in PSC-BTC have identified frequent alterations in *TP53* and *KRAS* and a tier of less frequent alterations in other genes found in multiple cancer types, including *CDKN2A*, *SMAD4*, *PIK3CA*, and *ERBB2*.[7,8] In unbiased sequencing efforts in BTC, limitations in the numbers of included PSC-BTC cases ($n < 5$) have precluded further conclusions on the genomic architecture of this BTC subtype.[9]

In this study, we performed whole-exome sequencing of a large, well-characterized formalin-fixed, paraffin-embedded (FFPE) tissue panel to identify relevant somatic mutations and copy number variations (CNVs) in PSC-BTC. Our results provide a basis for a better understanding of the molecular pathogenesis of PSC-BTC and highlight potential biomarkers for prognosis and individualized treatment in PSC-BTC.

METHODS

Tissue samples and clinicopathological data

Archived FFPE tissue specimens sampled for diagnosis or treatment of PSC-BTC during the period of 2000–2014 were collected, comprising diagnostic biopsies and surgical specimens. A total of 54 PSC-BTC samples were included from the University Hospitals in Hannover (n = 23) and Heidelberg (n = 10), Germany, and Oslo (n = 21), Norway. The PSC diagnosis was based on standard clinical, biochemical, cholangiographic, and histological criteria. The diagnoses of CCA and gallbladder carcinoma were established by histopathological and radiological evaluation.[4] Two board-certified hepatobiliary pathologists (Benjamin Goeppert and Peter Schirmacher) validated the diagnoses, histopathology, and tumor grading. Tumor staging was done according to the American Joint Committee on Cancer classification (AJCC, 8th Edition). After histomorphological and technical quality control, 2 samples were excluded: 1 due to low DNA quality and 1 due to a low amount of paired normal tissue; the final panel submitted to further mutational profiling therefore consisted of 52 PSC-BTC tissue specimens (Figure 1). Clinical and histopathological information at baseline was available for all 52 patients (Table 1).

Ethical approval

Written informed consent was obtained from all study subjects. Study protocols were approved by the regional committee for medical and health research ethics South-Eastern Norway (2015/736 28290) and the ethical board of the Hannover Medical School, Hannover, Germany (940-2011). For the use of long-time archived samples, an exemption from informed consent was obtained by the ethical board of the University Hospital Heidelberg, Germany (206/05) to allow the use of the samples.

All research was conducted in accordance with both the Declarations of Helsinki and Istanbul.

Isolation of genomic DNA

Tumor and paired nontumor tissue were isolated and transferred to RNase-free and DNase-free tubes.

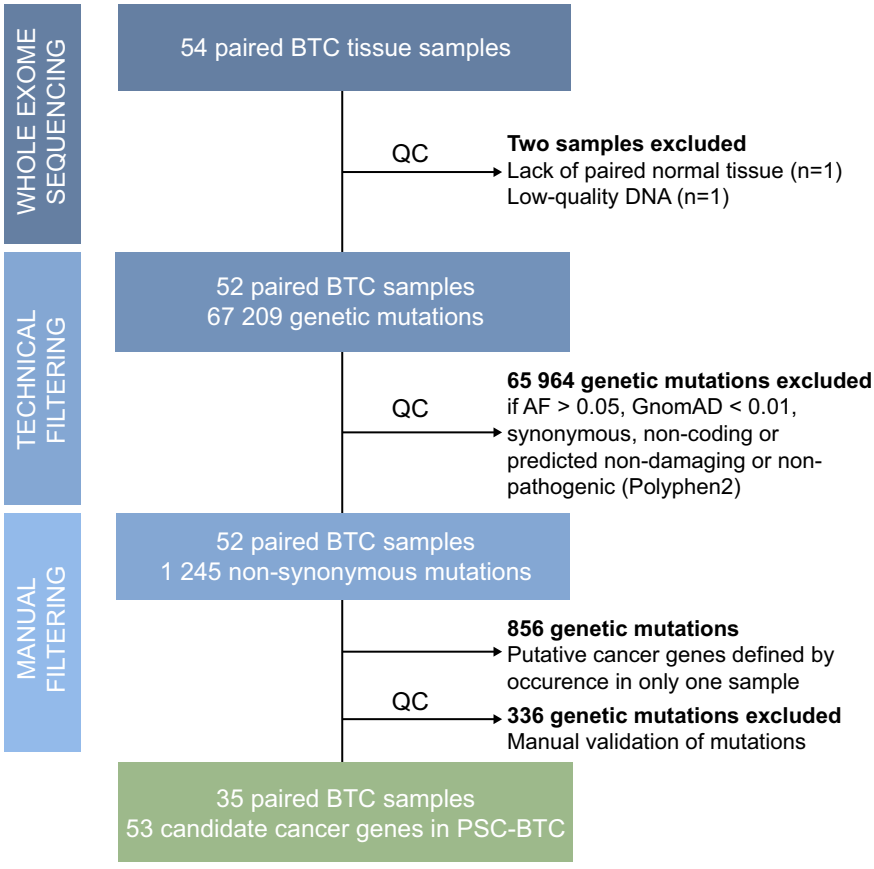

FIGURE 1 Schematic overview of the study design and filtering process of whole-exome sequencing data in PSC-associated biliary tract cancers (created with BioRender.com). For details regarding manual validation of mutations, see Methods and Supplemental Methods, http://links.lww.com/HC9/A933. Abbreviations: AF, technical allele frequency; BTC, biliary tract cancer; GnomAD, The Genome Aggregation Database; Polyphen2, Polymorphism Phenotyping v2; PSC, primary sclerosing cholangitis; QC, quality control.

TABLE 1 Clinical and histopathological data of the PSC-associated biliary tract cancer cohort (n = 52)

Mean age at BTC diagnosis (range)	49.6 y (22.7–75.5)
Mean age at PSC diagnosis[a] (range)	43.4 y (17.1–71.2)
Median time from PSC to BTC diagnosis (range)	35.5 mo (0.0–431.1)
Sex, n (%)	
Male	40 (76.9)
Female	12 (23.1)
Type of PSC[b], n (%)	
Large duct PSC	52 (100)
Small duct PSC	0 (0)
Inflammatory bowel disease (IBD), n (%)	
Ulcerative colitis	33 (63.5)
Crohn's disease	1 (1.9)
Indeterminate colitis	2 (3.8)
No IBD	16 (30.8)
Dead (at the last date of follow-up), n (%)	
Yes	42 (80.8)
No	8 (15.4)
Unknown	2 (3.8)
Cause of death (% of total number of dead = 42), n (%)	
Not PSC-related	0 (0)
Related to PSC-malignancy	7 (16.7)
Other PSC complication	1 (2.4)
Unknown	34 (81.0)
Liver transplanted, n (%)	21 (40.4)
Sampling procedure, n (%)	
Biopsy	3 (5.8)
Resection	35 (67.3)
Liver transplantation	13 (25.0)
Unknown	1 (1.9)
Origin of tumor sample, n (%)	
Primary tumor	45 (86.5)
Regional metastasis	5 (9.6)
Distant metastasis	2 (3.8)
Anatomical location of primary tumor, n (%)	
Intrahepatic[c] cholangiocarcinoma	19 (36.5)
Extrahepatic cholangiocarcinoma[d]	19 (36.5)
Gallbladder carcinoma	13 (25.0)
Unclear location of cholangiocarcinoma	1 (1.9)
Histology, n (%)	
Not otherwise specified (NOS)[e]	22 (42.3)
Papillary	7 (13.5)
Mucinous	9 (17.3)
Solid	9 (17.3)
Diffuse	4 (7.7)
Adenosquamous	1 (1.9)
AJCC (8th edition), n (%)	
AJCC 0	2 (3.8)
AJCC 1	3 (5.8)
AJCC 2	6 (11.5)
AJCC 3	19 (36.5)
AJCC 4	12 (23.1)
NA	10 (19.2)
pT, n (%)	
Tis	2 (3.8)
T1	4 (7.7)
T2	17 (32.7)
T3	16 (30.8)
T4	3 (5.8)
NA	10 (19.2)
pN, n (%)	
N0	16 (30.8)
N1	24 (46.2)
NA	12 (23.1)
M, n (%)	
M0	34 (65.4)
M1	12 (23.1)
NA	6 (11.5)
G, n (%)	
G1	4 (7.7)
G2	33 (63.5)
G3	3 (5.8)
NA	12 (23.1)
R, n (%)	
R0	3 (5.8)
R1	2 (3.8)
R2	1 (1.9)
NA	46 (88.5)

Note: Percentages rounded to the first decimal.
[a]Two patients had missing age at PSC diagnosis.
[b]Two patients had large duct PSC with features of autoimmune hepatitis.
[c]The intrahepatic cholangiocarcinomas were all of a large duct histology subtype.
[d]Perihilar and distal cholangiocarcinoma.
[e]Typical ductal/glandular/tubular/acinar histologic phenotype of biliary tract cancer.
Abbreviations: AJCC, American Joint Committee on Cancer; AJCC 0-4, American Joint Committee on Cancer stages 0–4; BTC, biliary tract cancer; G, grade of differentiation; L/V, invasion into lymphatic vessels/veins; M, distant metastases; pN, histopathologic lymph node evaluation; Pn, perineural invasion; PSC, primary sclerosing cholangitis; pT, histopathologic tumor stage evaluation; R, resection margins; Tis, carcinoma in situ.

Genomic DNA was extracted with the Maxwell 16 FFPE Plus LEV DNA Purification Kit (Promega). See Supplemental Methods, http://links.lww.com/HC9/A933 for details.

Library preparation and exome sequencing

To minimize bias from potential FFPE artifacts, tumor DNA samples were prepared in duplicates using 2 different preparation libraries, Illumina TruSight

Oncology and Illumina TruSeq Nano, and sequenced on an Illumina NovaSeq S4 (see Supplemental Methods, http://links.lww.com/HC9/A933 for further details) with 2×100bp paired-end sequencing, to 100×, 166× or 250× depth per library for tumor contents of ≥50%, 30%–49%, and <30%, respectively. Nontumor DNA was sequenced to 50× on-target depth (see Supplemental Methods, http://links.lww.com/HC9/A933). In addition, whole-genome sequencing of tumor and paired nontumor DNA, with a median coverage of 0.15×, was performed for CNV calling.

Somatic mutation calling, filtering, and variant analysis

Somatic variants were called using VarDict.[10] Nonsynonymous variants present in both tumor libraries were first filtered based on minimum coverage (10 reads), base quality (≥20), and allele frequency (AF) (>0.05) and assigned with *p* values and technical AFs using the pibase software[11] and annotated using ANNOVAR.[12] Annotated variants were submitted to second filtering, including only variants with a *p* value <0.05, technical AF >0.05, and a Genome Aggregation Database[13] AF <0.01 (Figure 1). Somatic variants in recurrently affected genes, defined by occurrence in 2 or more patients, were further subjected to functional filtering based on the prediction of the impact of nonsynonymous amino acid changes (see Supplemental Methods, http://links.lww.com/HC9/A933). Lastly, somatic variants representing potential artifacts were excluded based on manual inspection using the Integrative Genomics Viewer[14] and publicly available resources of erroneous sequences (see Supplemental Methods, http://links.lww.com/HC9/A933). Recurrent genes with somatic variants passing these filtering steps were defined as candidate cancer genes (Figure 2), whereas the remaining nonrecurrent genes, occurring only in 1 patient (1/52, 1.9%), were defined as putative cancer genes (see Supplemental Table S1, http://links.lww.com/HC9/A934).

CNVs were called using QDNAseq with a bin size of 200 kb and annotated according to the QDNAseq Manual. After the initial identification of 744 CNVs, potential erroneous large fragment-sized CNVs >5 Mb were excluded. Further analysis included 26 adjacent regions of focal and overlapping CNVs ≤5 Mb (Figure 3B). See Supplemental Methods, http://links.lww.com/HC9/A933 for the selection strategy of candidate genes within CNV regions, in the following referred to as CNV-affected genes.

Pathway and interaction analysis

The TCGA pan-cancer pathways[15] and a search in PubMed were used for pathway annotation of the identified candidate cancer genes (Supplemental Table S2, http://links.lww.com/HC9/A933) and the CNV-affected genes (Supplemental Table S3, http://links.lww.com/HC9/A934). All candidate cancer genes, nonrecurrent putative cancer genes, and CNV-affected genes were compared to the CiliaCarta[16] and SysCilia[17] databases of genes associated to ciliary function. The search tool for retrieval of interacting proteins (STRING) was applied to the list of genes identified using these 2 cilia databases, to predict functional interactions of proteins.[18]

Possible actionable target genes

Possible actionable target genes were identified using the TARGET (tumor alterations relevant for genomics-driven therapy) database version 3 from Broad Institute[19] and My Cancer Genome (database of ongoing clinical trials for targeted cancer therapies[20] (Supplemental Table S4, http://links.lww.com/HC9/A933).

Immunohistochemical staining and chromogen-in-situ-hybridization

Tissue microarrays (TMAs) were fabricated previously for 95 PSC-BTC specimens[7]; of these 51 specimens were submitted to exome sequencing in this study.

For immunohistochemical (IHC) staining and chromogen-in-situ-hybridization (CISH), TMAs were cut and stained according to the protocol. Staining intensity and percentage of positive cells were scored, and CISH for *MDM2* gene amplification was performed according to the protocol (for further details, see Supplemental Methods, http://links.lww.com/HC9/A933).

Results from IHC staining and CISH for Her2, EGFR, c-Met, c-Myc, PD-L1, and microsatellite instability and from targeted sequencing of an *FGFR2* fusion panel were available from a previous publication.[7]

Statistical analysis

The distribution, frequency, and co-occurrences of genomic alterations were visualized using the computing environment R (Supplemental Methods, http://links.lww.com/HC9/A933). Survival analyses are described in Supplemental Methods, http://links.lww.com/HC9/A933. Publicly available sequencing data of 412 BTC samples by Wardell et al[21] was analyzed for the candidate cancer genes in PSC-BTC (see Supplemental Table S5, http://links.lww.com/HC9/A933).

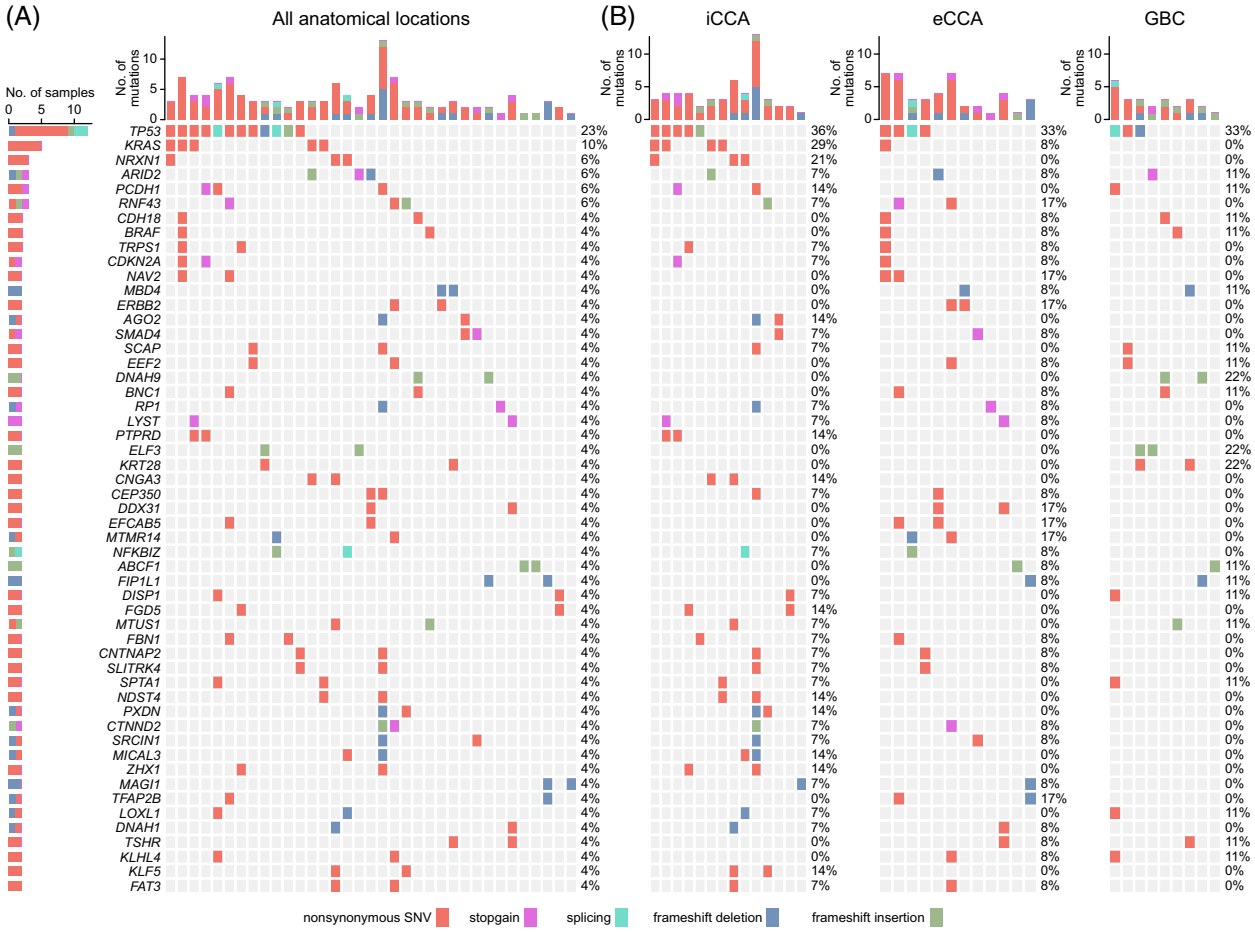

FIGURE 2 Recurrent somatic mutations in PSC-associated biliary tract cancer. Somatic mutation pattern of the 53 recurrently mutated candidate cancer genes in PSC-associated BTC from whole-exome sequencing of 35 tumors. Each row represents a somatic candidate cancer gene and each column represents an individual PSC-BTC tumor sample. Horizontal bar graphs show the total number of somatic mutations within the respective genes. (A) Recurrent mutations across all anatomical subtypes of BTC. (B) Recurrent mutations in iCCAs, eCCAs, and GBCs. Abbreviations: BTC, biliary tract cancer; eCCA, extrahepatic cholangiocarcinoma; GBC, gallbladder carcinoma; iCCA, intrahepatic cholangiocarcinoma; PSC, primary sclerosing cholangitis; SNV, single-nucleotide variant.

RESULTS

Clinical and histopathological characteristics of the PSC-BTC patient cohort

Tumor and paired nontumor tissue from 52 patients with underlying large duct PSC-associated BTC, including 19 intrahepatic CCAs (iCCAs), 19 extrahepatic CCAs, 13 gallbladder carcinomas, and 1 CCA with unclear anatomical origin were successfully evaluated (Table 1). The majority of samples (48/52, 92.3%) were obtained from liver resections (35/52, 67.3%) and liver explant samples (13/52, 25.0%) with a predominance of moderate grade (33/52, 63.5%) and ductal/glandular/tubular/acinar (=NOS [not otherwise specified]) (22/52, 42.3%) adenocarcinomas (Table 1). None of the iCCAs (n = 19) had features of cholangiolar/small duct histology, that is, all iCCAs were of the large duct histology subtype. Most tumors were AJCC stage 3-4 (41/52, 78.7%). The PSC-BTC cohort showed a male preponderance (40/52, 76.9%) and the mean ages at diagnoses of PSC and BTC were 43.4 (range: 17.1–71.2) and 49.6 years (range: 22.7–75.5), respectively (Table 1).

Exome sequencing and CNV analysis of PSC-BTC identify both novel and known candidate cancer genes

Median sequencing depth was 166× in tumor tissue and 50× in paired nontumor tissue. The median tumor mutation burden was 1.86 mutations/Mb. C to T and G to A transitions represented the most frequent mutation in all anatomical subtypes of PSC-BTC.

In 35 (67.3%) of the 52 PSC-BTC samples analyzed by whole-exome sequencing (Figure 1), we identified 53 recurrently mutated genes, represented by 123 nonsynonymous somatic variants, mainly including single-nucleotide variants (66.7%) and frameshift insertions or deletions (24.0%) (Figure 2). In total,

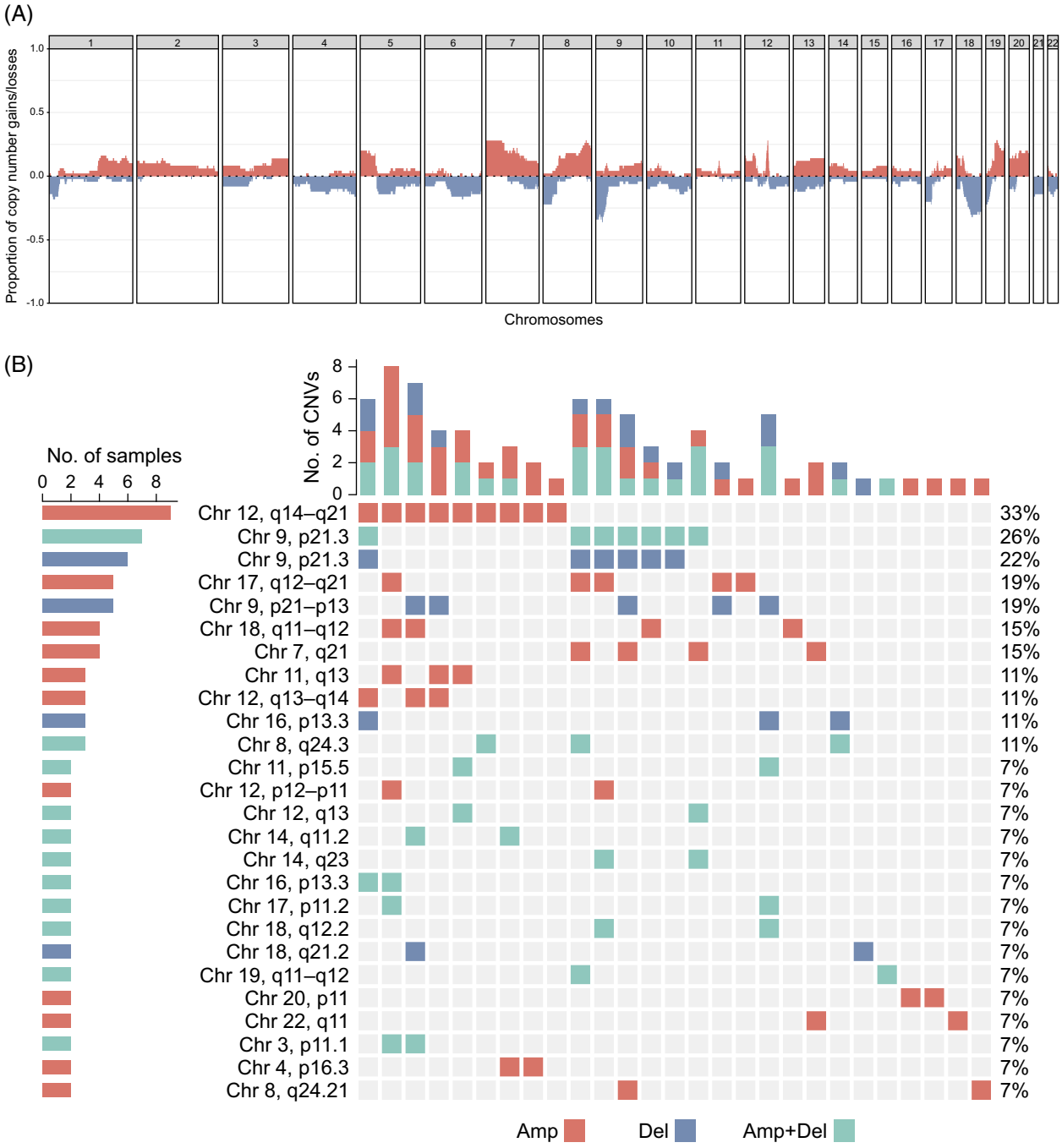

FIGURE 3 Copy number variations in PSC-associated biliary tract cancer. (A) Genome-wide frequency plot of copy number aberrations in 52 PSC-associated BTC tumors. Frequencies of gains/amplifications are marked in red and losses/deletions are marked in blue. (B) Oncoplot of the distribution of focal copy number variants in PSC-BTC. Each row represents a chromosomal region, each column represents an individual PSC-BTC tumor, and each colored square indicates an amplification (red), deletion (blue), or a combination of amplifications and deletions within the same region (green). See Supplemental Table S8 for details, http://links.lww.com/HC9/A934. Abbreviations: Amp, amplification; BTC, biliary tract cancer; Chr, chromosome; CNV, copy number variation; Del, deletion; PSC, primary sclerosing cholangitis.

10/53 (18.9%) of the identified recurrently mutated genes have to our knowledge not previously been robustly associated with BTC, including *CEP350*, *CNGA3*, *CNTNAP2*, *EFCAB5*, *KRT28*, *LYST*, *MICAL3*, *RP1*, *SCAP*, and *SLITRK4*. Within the tumor samples these novel genes all co-occurred with genes previously implicated in BTC or other cancers (Supplemental Table S6, http://links.lww.com/HC9/A934). The clinical characteristics of the 13 patients with PSC-BTC harboring these novel genes did not display any significant differences when compared to the rest of the cohort (Supplemental Table S7, http://links.lww.com/HC9/A933). A second subset of 6/53 (11.3%) comprised genes previously implicated in hepato-pancreato-biliary

TABLE 2 Candidate genes located within regions of focal copy number variations in PSC-associated biliary tract cancer

Region name	Chromosome	Coordinates	Cytoband	Candidate genes in region	Number of patients, n (%)
A: Amplified regions					
Chr 4, p16.3	4	600,000–2,200,000	p16.3	*CTBP1, FGFR3, NSD2*	2 (3.8)
Chr 7, q21	7	81,800,000–93,600,000	q21.11, q21.2, q21.3	*TFPI2, SEMA3A, SEMA3E*	4 (7.7)
Chr 8, q24.21	8	128,400,000–128,800,000	q24.21	*MYC*	2 (3.8)
Chr 11, q13	11	69,000,000–70,600,000	q13.3, q13.4	*ANO1, CCND1, CTTN, FADD, FGF19, FGF3, FGF4, MIR548K, PPFIA1*	3 (5.8)
Chr 12, p12-p11	12	26,000,000-28,200,000	p12.1, p11.23, p11.22	*KLHL42*	2 (3.8)
Chr 12, q13-q14	12	56,000,000–58,400,000	q13.2, q13.3, q14.1	*CDK2, DTX3, NAB2, STAT6*	3 (5.8)
Chr 12, q14-q21	12	64,200,000–72,400,000	q14.2, q14.3, q15, q21.1	*MDM2, LGR5*	9 (17.3)
Chr 17, q12-q21	17	34,800,000–39,200,000	q12, q21.1, q21.2	*ERBB2, LASP1, IKZF3, CCR7*	5 (9.6)
Chr 18, q11-q12	18	18,600,000–26,400,000	q11.1, q11.2, q12.1	*SS18, ZNF521*	4 (7.7)
Chr 20, p11	20	21,800,000–22,800,000	p11.22, p11.21	*FOXA2*	2 (3.8)
Chr 22, q11	22	17,200,000–21,200,000	q11.1, q11.21	*CLTCL1, DGCR8*	2 (3.8)
B: Deleted regions					
Chr 9, p21.3	9	21,000,000–22,000,000	p21.3	*CDKN2A, CDKN2B*	6 (11.5)
Chr 9, p21-p13	9	29,000,000–34,600,000	p21.1, p13.3	*LINC01243*	5 (9.6)
Chr 16, p13.3	16	200,000-2,000,000	p13.3	*AXIN1*	3 (5.8)
Chr 18, q21.2	18	48,400,000-49,000,000	q21.2	*SMAD4*	2 (3.8)

Note: For regions containing both amplifications and deletions, see Supplemental Table S8 for details, http://links.lww.com/HC9/A934.
Abbreviation: Chr, Chromosome.

cancer, including *ARID2*, *DNAH1*, *ELF3*, *PTPRD*, *SPTA1*, and *ABCF1* (Supplemental Table S8, http://links.lww.com/HC9/A934). Comparisons with the data set from Wardell et al, including 412 BTC from diverse etiologies (predominantly non-PSC), showed that 67.9% (36/53) of the hereby implicated PSC-BTC genes overlap with identified driver genes from the Wardell publication (Supplemental Table S5, http://links.lww.com/HC9/A933).[21] When comparing the candidate cancer genes identified in our PSC-BTC cohort with that of extrahepatic eCCAs included in Jusakul et al, we found that the majority of genes identified in our study were not present or only present at low frequencies in the Jusakul et al cohort (Supplemental Figure S4, http://links.lww.com/HC9/A933).[22] For the most frequently mutated genes in our data, *TP53* and *KRAS*, however, the frequency was slightly higher in the Jusakul et al panel for non-PSC BTC. In our data set, we found a higher frequency of the potentially targetable genes, *BRAF*, *CDKN2A*, and *RNF43*, compared to the Jusakul et al data set.

Finally, we also identified 37/53 (69.8%) genes implicated in several cancers such as tumor suppressor genes *TP53*, *CDKN2A*, *SMAD4*, and *RNF43* and the oncogenes *KRAS*, *ERBB2*, and *BRAF*.[23,24] For details and functional annotation of the 53 candidate cancer genes in PSC-associated BTC, see Supplemental Tables S8, http://links.lww.com/HC9/A934 and S9, http://links.lww.com/HC9/A934.

Of note, in the 19 cases of intrahepatic PSC-BTC, we did not observe genomic alterations in *IDH1*, *IDH2*, *BAP1*, or *FGFR2*, all of which are characteristic of small duct-type iCCA.[22]

The number and diversity of genes implicated in PSC-BTC are likely to extend beyond the herein-defined 53 genes, exemplified by the 856 additional putative cancer genes in PSC-BTC, identified in only 1 tumor sample in this study (Supplemental Table S1, http://links.lww.com/HC9/A934). In 12 patients (23.0%), we found nonrecurrent mutations only, and in 5 patients (9.6%) no genomic alterations passing initial filtering

thresholds were discovered. Comparing the clinicopathological data for these 2 groups with the patients with recurrently mutated genes, we observed a significantly higher frequency of the NOS histology subtype tumors and specimens sampled from regional/distant metastases in the group with no qualifying alterations (Supplemental Table S10, http://links.lww.com/HC9/A934).

Our cohort consisted of 11 patients with early-stage tumors (AJCC 0–2) and 31 patients with late-stage tumors (AJCC 3–4). The following genes were only found mutated in early-stage tumors: *MTMR14*, *SLITRK4*, *ERBB2*, *ABCF1*, *CNTNAP2*, and *CTNND2*. These should be further examined for their potential as early detection markers in PSC-BTC (Supplemental Table S11, http://links.lww.com/HC9/A933).

In addition, whole-genome sequencing identified CNVs in 27/52 (51.9%) of the tumors, all of which also harbored nonsynonymous somatic variants within the PSC-BTC candidate cancer genes (Table 2, Supplemental Table S12, http://links.lww.com/HC9/A934 and Figure 3). A subset of these CNV regions has not been reported in BTC previously, including focal CNVs at chr19q11-q12 and chr18q12.2. The remaining CNVs contained genes with known association to several cancers (eg, *FGFR3*, *MYC, FADD*, and *LASP1* [for annotation of CNV-affected genes, see Supplemental Table S3, http://links.lww.com/HC9/A934]). The most frequent CNV was an amplification at chromosome 12q14-q21 occurring in 9/52 tumors (17.3%), which has previously been implicated in sporadic BTC, comprising the TP53 pathway oncogene *MDM2* (Table 2).[15,25]

Annotation of candidate PSC-associated BTC cancer genes and CNV-affected genes implicates pan-cancer pathways and ciliary signaling pathways

We annotated the 53 PSC-BTC candidate cancer genes using the TCGA pan-cancer pathways[15] and found that 50.9% (27/53) of the genes were implicated in hallmark cancer pathways, including the PI3K pathway (8/53, 15.1%), WNT pathway (8/53, 15.1%), TP53 pathway (4/53, 7.5%), RTK/RAS pathway (3/53, 5.7%), HIPPO pathway (2/53, 3.8%), cell cycle pathway (1/53, 1.9%), and TGF-beta pathway (1/53, 1.9%) (Figure 4A and Supplemental Table S2, http://links.lww.com/HC9/A933). Co-occurrence of pathways was commonly seen for the TP53 and the P13K pathway (8/52 tumors, 15.4%) and the TP53 and WNT pathway (4/52 tumors, 7.7%) (Figure 4B). Mutual exclusiveness of the RTK/RAS and WNT pathway affection was frequent (~80%), similar to what has been observed in pancreatic cancer and sporadic BTC.[26] (Figure 4A). A similar pattern was observed for the candidate genes in the CNV regions, where 48.1% (26/54) converged into the same canonical cancer pathways (Supplemental Table S3, http://links.lww.com/HC9/A934).

In the functional annotation process of the candidate cancer genes, we discovered that several genes were associated with primary cilia function. We therefore performed formal annotation to pathways implicated in ciliary function using CiliaCarta[16] and SysCilia.[17] This showed that 9.4% (5/53) of the candidate cancer genes (*RP1*, *DNAH1*, *DNAH9*, *CNGA3*, and *NRXN1*), 37% (20/54) of the CNV-affected genes (eg, *CABYR*, *ODF3*, *STK38L*, and *CCDC78*), and multiple putative cancer genes may be involved in primary cilium function and ciliary signaling (Supplemental Table S13, http://links.lww.com/HC9/A933). Furthermore, STRING interaction analysis showed frequent interactions between these cilia-associated genes (Figure 5).

Lastly, a subset of PSC-BTC candidate cancer genes was associated with other known signaling pathways in cancer, including the hedgehog pathway (eg, *DISP1*),[27] chromatin remodeling, and transcription modifying pathways (eg, *ARID2, TFAP2B*, and *ZHX1*).[28,29] A total of 22/53 (41.5%) of the PSC-BTC genes could not be assigned to any established signaling pathway in cancer (Supplemental Table S2, http://links.lww.com/HC9/A933).

Prognostic value of candidate cancer genes and pathways in PSC-associated BTC

The median overall survival was 19.5 months and the 5-year survival rate was 18.8% (Supplemental Figure S1, http://links.lww.com/HC9/A933). Alterations within *KRAS* ($p = 0.0014$) (Supplemental Figure S2, http://links.lww.com/HC9/A933) and in genes within the RTK/RAS pathway ($p = 0.036$), TP53 pathway ($p = 0.040$), and PI3K pathway ($p = 0.043$) were associated with significantly shorter overall survival (Supplemental Figure S3, http://links.lww.com/HC9/A933). As we observed frequent co-occurrence of the TP53 and PI3K pathways ($n = 7$), survival analysis for this subgroup was performed which also revealed a significantly decreased survival ($p = 0.0082$). Overall survival was worse for patients with late AJCC stage (3–4) compared to early stage (0–2) ($p = 0.027$). Conversely, when stratifying patients by tumor mutational burden (≥ 2 mutations/Mb vs. <2 mutations/Mb), we found no significant difference in overall survival ($p = 0.59$).

Putative actionable genes in PSC-associated BTC

Among the 53 PSC-BTC candidate cancer genes, 8 (15.1%) are currently considered actionable according to the TARGET[19] and My Cancer Genome databases

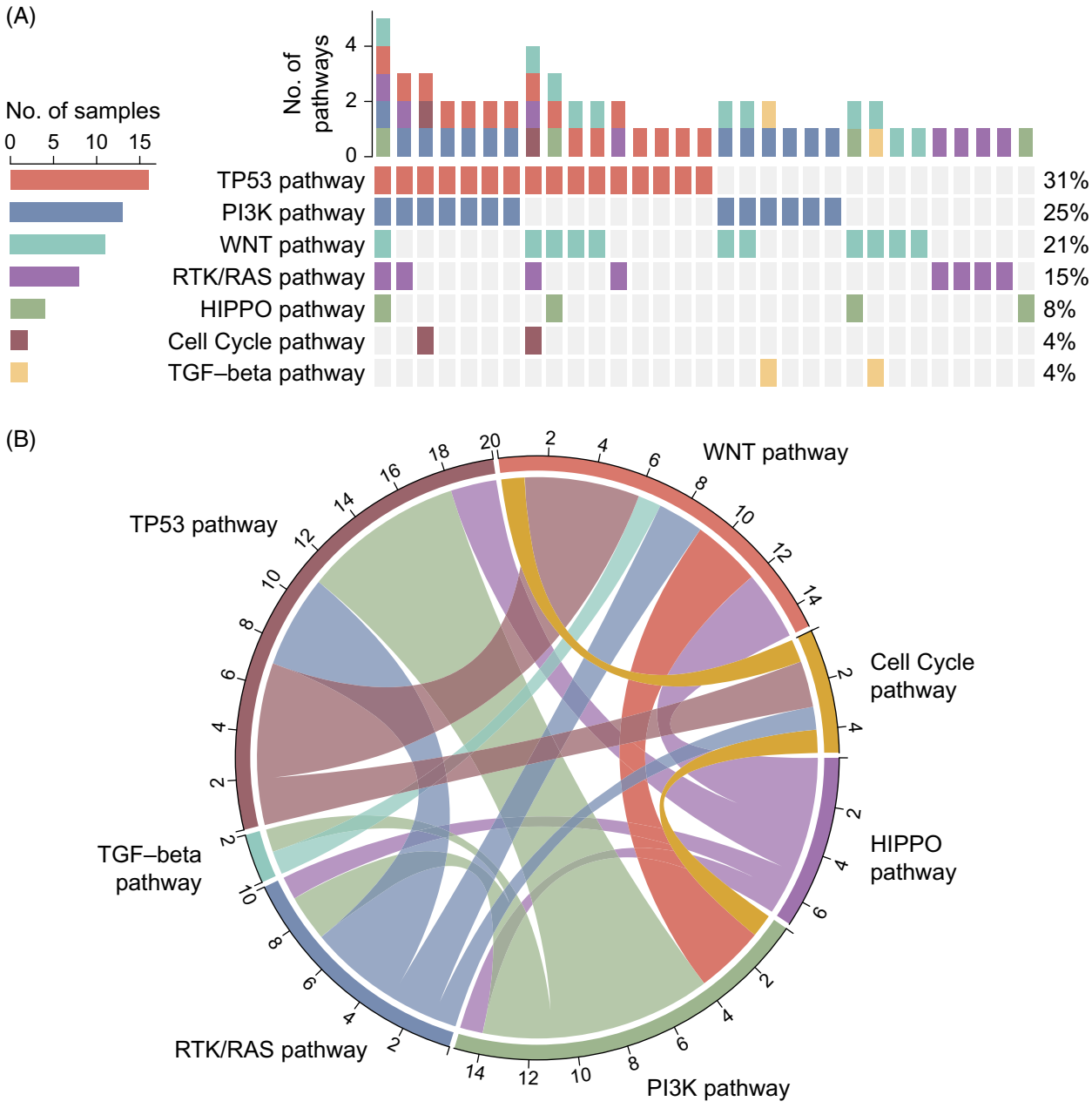

FIGURE 4 Distribution and co-occurrence of somatic candidate cancer mutations in PSC-associated biliary tract cancer by categorization into canonical cancer pathways. (A) Oncoplot showing the distribution of somatic candidate cancer mutations in PSC-BTC by annotation to canonical cancer pathways. Each row represents a cancer pathway and each column represents an individual tumor sample. Somatic candidate cancer mutations without established annotation to canonical cancer pathways were omitted from this plot. (B) Circos plot representing the co-occurrence of canonical cancer pathways. A band connecting pathways represents co-occurring pathways in a given tumor sample. The width of the band represents the frequency of this pathway pair within the data set (for categorization of genes into canonical pathways, see Supplemental Table S2, http://links.lww.com/HC9/A933). Abbreviations: BTC, biliary tract cancer; PI3K, phosphatidylinositol-3-kinase; PSC, primary sclerosing cholangitis; RAS, rat sarcoma; RTK, receptor tyrosine kinase; TP53, tumor protein 53; WNT, wingless-related integration site.

(Supplemental Table S4A, http://links.lww.com/HC9/A933).[20] In *KRAS*, the G12D mutation predominated (80%), for which specific inhibitors are being evaluated for solid tumors in phase 1 (NCT05737706 and NCT06227377) but no G12C mutations, for which specific inhibitors have been approved, were identified in this cohort. The mutations in *BRAF* were of the non-V600E type (G469E and D594G) for which EGFR and MEK inhibitors may be effective.[30] In *ERBB2*, 2 missense substitutions were identified (L841 and S310F) for which there are ongoing and finalized phase 2 studies evaluating these alterations in breast cancer and BTC, respectively (eg, NCT02673398 and NCT04579380).[31] Consistent with European non-PSC-CCA, no microsatellite instability–high or c-Myc–positive tumors were identified,[7,32] but EGFR protein

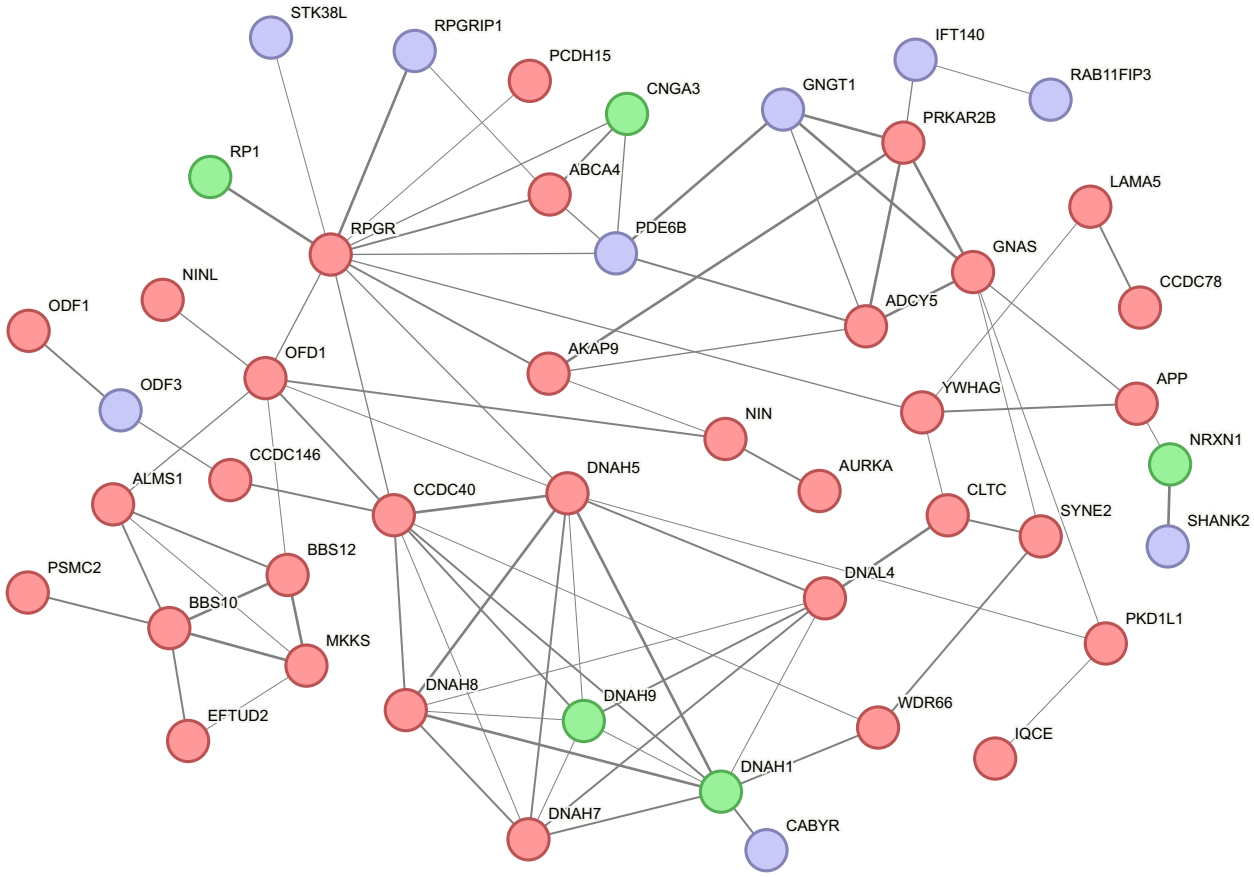

FIGURE 5 Protein-protein interaction networks for PSC-associated biliary tract cancer candidate cancer genes with established association to ciliary function. STRING analysis derived protein-protein interaction networks for the proteins expressed by recurrent somatic candidate cancer genes (green nodes), CNV-associated genes (blue nodes), and putative cancer genes (red nodes) in PSC-associated BTC: A line between 2 proteins indicate predicted protein-protein interactions. The thickness of the line indicates the strength of the correlation. The interaction lines are based on co-expression, co-occurrence, gene fusion, neighborhood, databases, experiments, and text mining. The minimum required interaction score is 0.4 (medium confidence). Proteins with no interactions have been removed from the plot. Abbreviations: BTC, biliary tract cancer; CNV, copy number variation; Del, deletion; PSC, primary sclerosing cholangitis; STRING, search tool for the retrieval of interacting proteins.

expression was observed in 22/49 (44.9%), c-Met in 7/50 (14.0%), and for PD-L1 in 9/48 (18.8%) by IHC staining (Supplemental Table S14, http://links.lww.com/HC9/A933).

In addition, 10 chromosomal regions had CNVs that included genes reported to be actionable, for example, *MDM2*, *ERBB2*, *FGFR3*, *CDKN2B*, and *CCND1* (Supplemental Table S4B, http://links.lww.com/HC9/A933). Amplifications of *MDM2* occurred in 17.3% of the PSC-BTC tumors based on sequencing data (Figure 6A). As CISH is the gold standard for detecting high-level amplification, we performed CISH analysis of *MDM2* using previously prepared TMAs on 51 of the tumor samples included in the actual study and an additional independent cohort of 44 PSC-BTC tumors (Figures 6B, C). *MDM2*-CISH revealed that 7 (7/95, 7.4%) of PSC-BTC tumors had high-level amplification which all also exhibited high MDM2 protein expression (IRS 8 or 12, Figure 6D). Consistently, tumors that did not exhibit *MDM2* amplification by CISH analysis had intermediate to absent MDM2 expression (Figure 6D). Interestingly, p53 protein expression was neither activated nor reduced in tumors with *MDM2* gene amplification as all 7 tumors showed p53 wildtype expression. Loss of p53 expression was observed in 26/81 (32.1%) of samples of which 4 had frameshift or splice-side mutations. Furthermore, *ERBB2* amplification was detected in 5/51 (9.8%) of the samples by whole-exome sequencing (Figure 6A) and in 8/95 (8.4%) of cases by CISH (Figure 6D). Coamplification of *EGFR* and *ERBB2* has been reported to impact the therapeutic efficacy of chemotherapy, radiotherapy, and hormonal therapy.[33] In our data, coamplification of *EGFR* and *ERBB2* was found in 1 out of 5 tumors positive for *ERBB2* by IHC and CISH (Supplemental Table S15, http://links.lww.com/HC9/A933).

DISCUSSION

To delineate the genomic architecture of PSC-associated BTC, we performed whole-exome sequencing for

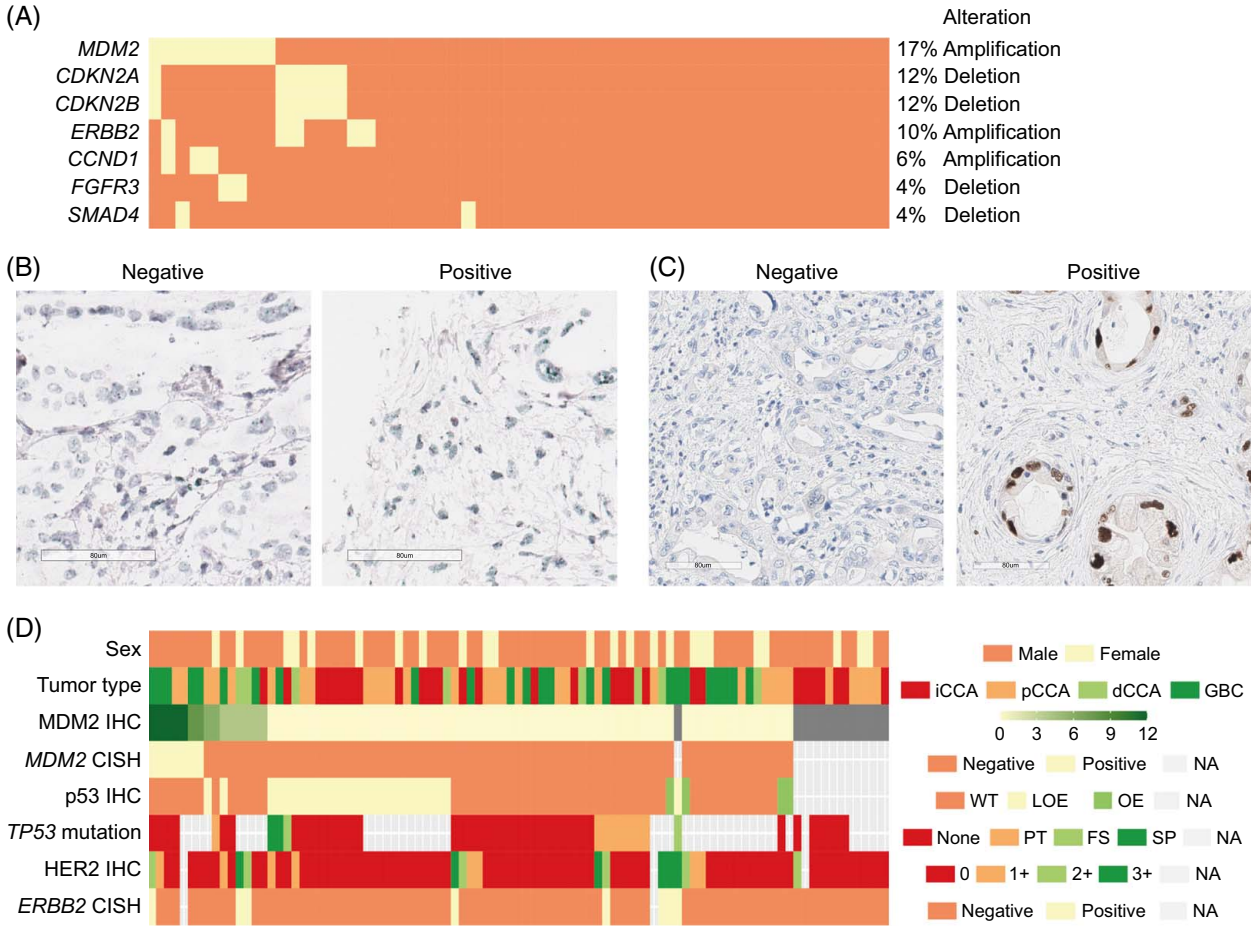

FIGURE 6 Genomic alterations and alteration of the MDM2 and p53 pathways in PSC-associated BTC. (A) Heatmap of the distribution of CNV of potentially therapeutic relevant genes in PSC-BTC. Each row represents a gene, each column represents an individual PSC-BTC tumor, and each colored square indicates an alteration (yellow) or unaltered genes (orange). (B) Representative image of a BTC case without (left panel) or with (right panel) MDM2 amplification observed by CISH. (C) Representative image of a BTC case without (left panel) or with (right panel) MDM2 protein expression detected by IHC. (D) Heatmap of MDM2, p53, and HER2 protein expression as well as MDM2 and HER2 amplification by CISH and TP53 mutation type. Abbreviations: CISH, chromogen-in-situ-hybridization; dCCA, distal cholangiocarcinoma; FS, frameshift mutation; GBC, gallbladder carcinoma; iCCA, intrahepatic cholangiocarcinoma; IHC, immunohistochemistry; LOE, loss of expression; NA, not available; OE, overexpression; pCCA, perihilar cholangiocarcinoma; PT, missense point mutation; SP, splice mutation; WT, wildtype.

somatic variants and genome sequencing for CNVs in a substantial panel of patients with PSC-BTC. We identified multiple novel candidate cancer genes, prognostic markers, and putative actionable targets in PSC-BTC. Our data demonstrated that CNVs are frequent genomic alterations in PSC-BTC occurring in ~50% of the characterized tumors. The absence of signature mutations for small duct-type iCCA in intrahepatic tumors from patients with PSC provides evidence that BTC in PSC represents a homogenous large duct subtype.

We identified 10 novel BTC candidate cancer genes, including *CEP350*, *CNGA3*, *CNTNAP2*, *EFCAB5*, *KRT28*, *LYST*, *MICAL3, RP1*, *SCAP*, and *SLITRK4,* some of which have not been directly implicated in any cancers previously. A subset of the identified CNV loci has also not been previously implicated in BTC. Prior knowledge of the pathogenic role of these novel cancer genes and CNV regions is limited, but suggestive evidence points to multiple relevant mechanisms in cancer, including RAB-mediated docking and fusion for cilia-directed vesicles and expansion of cancer stem–like cells (*MICAL3*),[34,35] cell autophagy (*LYST*),[36] epithelial cytoskeletal remodeling (*KRT28*),[37] and primary cilia function (eg, *CNGA3* and *RP1*).[16,17] Some of these newly identified loci may harbor functions specifically involved in BTC development in the context of PSC, but confirmation in independent cohorts and mechanistic studies will be needed to further explore their exact involvement.

We identified several additional cancer genes and CNVs implicated in sporadic BTC and/or other hepato-pancreato-biliary cancers previously, including somatic variants in *ARID2*, *DNAH1*, *ELF3*, *PTPRD*, *SPTA1*, and *ABCF1*, copy number amplifications in regions containing the oncogenes *MDM2*, *ERBB2*, *FGFR3*, *CCDN1*, and *MYC*, and deletions in tumor suppressors *CDKN2A* and *CDKN2B*. Our data also confirmed *TP53* and *KRAS*

as the predominant driver genes in PSC-BTC, together with the frequent amplifications of *MDM2* (17.3% of tumors). *MDM2* is of considerable interest in PSC-BTC since it is a critical regulator of tumor suppressor p53, particularly in circumstances of increased cellular inflammation and stress.[38] *MDM2* has previously been implicated in sporadic BTC,[25] but mostly at lower frequencies than we observe in our PSC-BTC cohort. Agents targeting the amplification of *ERBB2/HER2* have already been approved in BTC, while clinical trials using inhibitors targeting *FGFR3* and *MDM2* amplifications are ongoing.[39–41] A number of other pan-cancer driver genes, including *CDKN2A, SMAD4*, *ERBB2*, and *BRAF*, and CNVs at *SEMA3E*, *SS18*, and *AXIN1* were also identified.[42,43] Importantly, as these shared genomic alterations point to common mechanisms of carcinogenesis, they may open for the transferral of mechanistic and therapeutic insights from more prevalent cancers to the rare cancer setting represented by PSC-BTC.

Genomic alterations amenable to targeted therapy are a major unmet need in PSC-BTC, as BTC in these patients is often detected at advanced, noncurative stages with considerable resistance to standard palliative chemotherapy.[44] Even though our BTC cohort included a significant subset of early-stage tumors (~25% stage 0–2 tumors) and resection- or liver transplant cases (~90%), the extremely poor outcome for this group is reflected by the median survival of 19.5 months and the dismal 5-year survival rate of 18.8%, with outcomes being negatively impacted by alterations related to the RTK/RAS, the TP53, and PI3K pathways.

Of relevance for future treatment of people with PSC-associated BTC, we detected potentially actionable genes in a proportion of the tumors. Candidate PSC-BTC genes that are currently recognized as actionable in cancer include *ERBB2* and *FGFR3.* For *ERBB2*, accumulating data support a role for anti-*ERBB2* (Her2) targeted therapy in BTCs,[39] aimed at *ERBB2* amplifications, which were identified in our data. Inhibitors targeting mutations in *FGFR3* have been approved, while a series of clinical trials investigating drugs targeting *FGFR3* amplifications, as found in this study, are ongoing.[40] Furthermore, numerous small molecule *MDM2* inhibitors are currently undergoing clinical evaluation, including the study medicine BI 907828 in an ongoing phase II trial (NCT05512377) targeting *TP53* wildtype patients with BTC with *MDM2* amplifications.[41] Our IHC and CISH analyses performed on an extended cohort[7] also support a therapeutic potential for both *MDM2* inhibition and anti-*ERBB2* treatment in PSC-associated BTC. Other putative future targets in PSC-BTC include *KRAS*, where inhibitors for the G12C mutation have been developed, and a specific inhibitor against the G12D mutation, representing the most frequent *KRAS* mutation in our PSC-BTC cohort, is currently under development.[45] The dabrafenib and trametinib combination has been FDA-approved for BTCs with the class 1 *BRAF* V600E mutation; however, for the class 3 *BRAF* mutations G469E and D594G identified in our study, no targeted therapy has yet been approved.[46]

We provide robust evidence that PSC-associated BTC, also in cases of intrahepatic origin of the primary tumor (n = 19), represents a genetically homogenous large duct type BTC group with high mutation frequencies in *KRAS*, and the absence of *IDH1*, *IDH2*, and *BAP1* mutations and *FGFR2* fusions otherwise characteristic for small duct-type iCCA.[22] This observation has important implications, as large duct iCCAs are, contrary to small duct iCCAs, derived from mucin-producing columnar cholangiocytes and peribiliary glands and show a highly invasive periductal or intraductal growth frequently accompanied by a desmoplastic reaction.[47] Large duct–derived iCCAs have been associated with inferior response to palliative chemotherapy, poorer outcomes after curative intent treatment, and reduced overall survival compared to small duct–derived iCCAs.[48] Classification of iCCAs into large duct type in PSC may therefore impact clinical treatment planning and prognostic stratification.[48]

A notable feature in the current data is the accumulation of genomic alterations associated with the morphology and function of primary cilia. Close to 10% of the PSC-BTC candidate cancer genes and multiple CNV-affected genes are implicated in primary cilium function and signaling.[16,17] Loss of primary cilia in cholangiocytes has been implicated in previous studies in PSC and BTC, where the expression of deacetylases like HDAC6 has been observed to promote cilia loss and associated with dysregulation of the WNT, P13K, and hedgehog pathway in BTC progression.[49] Restoration of primary cilia by HDAC6 targeting and/or by using the short-chain fatty acid butyrate may therefore represent relevant therapeutic principles in PSC and PSC-BTC.[50]

This study has some principal limitations. Sequence artifacts and false-positive variant calls due to FFPE-related chemical modifications of the DNA represent known challenges for downstream processing and data analysis of FFPE-derived sequencing data. To avoid misclassification of variants, extensive quality control of the FFPE specimens and DNA, including the parallel application of 2 different preparation of libraries, together with rigorous data filtering and functional annotation, was performed. The scarcity of tumor material precluded direct evaluation of intratumor genetic heterogeneity. This is relevant for the interpretation of comparisons of the exome sequencing data with panel sequencing data performed on DNA extracted from neighboring areas of the same tumors in a previous study,[7] where we observed that a subset of low-frequency cancer genes identified in the targeted

sequencing effort (eg, *SMARCA4*, *FBXW7*, and *NRAS*) was not re-identified by exome sequencing (Supplemental Table S16, http://links.lww.com/HC9/A934). The lack of perfect concordance may reflect intratumor genetic heterogeneity in PSC-BTC[8] but could also result from under-ascertainment of variants due to technical aspects such as lower coverage depth and the filtering steps implicit to whole-exome sequencing. Although our study has a large sample size in the context of PSC-BTC, it is still low. As a result, it can be challenging to detect recurring mutations, and additional studies on independent patient cohorts should be conducted to evaluate the generalizability of our findings. Despite such limitations, the overall consistency of findings with previous publications in BTC and other cancers does not suggest major biases.

In conclusion, our study delineates both candidate PSC-specific and universal cancer genes that provide opportunities for a better understanding of biliary carcinogenesis in PSC. Overall, these findings may impact the clinical management of PSC-BTC, by serving as a platform to repurpose and develop personalized therapies utilizing the growing knowledge of actionable mutations.

AUTHOR CONTRIBUTIONS

Study concept and design: Andre Franke, Kirsten M. Boberg, Michael Forster, Trine Folseraas, and Tom H. Karlsen; acquisition of biological material and clinicopathological data: Alphonse Charbel, Arndt Vogel, Benjamin Goeppert, Krzysztof Grzyb, Kirsten M. Boberg, Michael P. Manns, Marit M. Grimsrud, Peter Schirmacher, Stephanie Roessler, Thomas Albrecht, Trine Folseraas, and Tom H. Karlsen; analysis and interpretation of data: Carmen Metzger, Georg Hemmrich-Stanisak, Irmi Sax, Michael Forster, Marit M. Grimsrud, Peder R. Braadland, Stephanie Roessler, Trine Folseraas, and Tim Alexander Steiert; drafting of the manuscript: Marit M. Grimsrud, Trine Folseraas, and Tom H. Karlsen; critical revision of the manuscript for important intellectual content: Benjamin Goeppert, Georg Hemmrich-Stanisak, Kirsten M. Boberg, Michael Forster, Marit M. Grimsrud, Matthias Schlesner, Peder R. Braadland, Stephanie Roessler, Sheraz Yaqub, Trine Folseraas, and Tom H. Karlsen; administrative, technical, or material support: Trine Folseraas and Tom H. Karlsen; study supervision: Trine Folseraas and Tom H. Karlsen. All authors have read and approved the final version of the manuscript.

ACKNOWLEDGMENTS

The authors are grateful to the Department of Pathology, Oslo University Hospital Rikshospitalet, for help with tissue sample selection and characterization. They also thank Liv Wenche Thorbjørnsen, Biobank manager, Norwegian Center for PSC Research, Oslo University Hospital Rikshospitalet, for logistical assistance. The authors very much appreciate Yewgenia Dolshanskaya's work on the NGS libraries. They thank the Tissue Bank of the National Center for Tumor Diseases (NCT) Heidelberg, Germany for TMA construction and Veronika Eckel and Fabio Tabone of the NCT Tissue Bank for technical assistance. They thank PSC Partners Seeking a Cure for their support of this study. This publication is based upon work from the European Network for the Study of Cholangiocarcinoma (ENS-CCA), the COST Action Precision-BTC-Network CA22125, supported by COST (www.cost.eu) and ERN Rare-Liver (www.rare-liver.eu)

FUNDING INFORMATION

This work was supported by a grant from The Bergesen Foundation and the Norwegian PSC Research Center. Marit M. Grimsrud was supported by the Helse Sør-Øst grant no. 2017016. Stephanie Roessler and Benjamin Goeppert were supported by funds from the PSC Partners Seeking a Cure Foundation USA, and Stephanie Roessler was in part supported by Deutsche Forschungsgemeinschaft (DFG, German Research Foundation), Project-ID 314905040—SFB/TRR 209 Liver Cancer, Project-ID 469332207 and Project-ID 493697503 and the German Cancer Aid (Deutsche Krebshilfe) project no. 70113922.

CONFLICTS OF INTEREST

Arndt Vogel consults for Roche. Tom H. Karlsen advises MSD, Albireo, and Falk, is on the speakers' bureau for Gilead, and owns stock in Ultimovacs. Peter Schirmacher consults, advises, is on the speakers' bureau, and received grants from Incyte. He consults, is on the speakers' bureau, and received grants from Bristol-Myers Squibb. He consults for MSD. The remaining authors have no conflicts to report.

ORCID

Marit M. Grimsrud https://orcid.org/0009–0004–6323–1807
Michael Forster https://orcid.org/0000–0001–9927–5124
Benjamin Goeppert https://orcid.org/0000–0002–4135–9250
Georg Hemmrich-Stanisak https://orcid.org/0000–0002–2896–4691
Krzysztof Grzyb https://orcid.org/0000–0002–2718–8125
Peder R. Braadland https://orcid.org/0000–0002–0794–7737
Alphonse Charbel https://orcid.org/0000–0002–7383–1898
Carmen Metzger https://orcid.org/0000–0001–7892–0235
Thomas Albrecht https://orcid.org/0000–0002–2234–0909
Tim Alexander Steiert https://orcid.org/0000–0002–0125–1173

Matthias Schlesner https://orcid.org/0000–0002–5896–4086
Michael P. Manns https://orcid.org/0000–0002–4485–8856
Arndt Vogel https://orcid.org/0000–0003–0560–5538
Sheraz Yaqub https://orcid.org/0000–0002–5696–2319
Tom H. Karlsen https://orcid.org/0000–0002–8289–9931
Peter Schirmacher https://orcid.org/0000–0002–0950–3339
Kirsten M. Boberg https://orcid.org/0000–0001–5567–9928
Andre Franke https://orcid.org/0009–0007–5603–4014
Stephanie Roessler https://orcid.org/0000–0002–5333–5942
Trine Folseraas https://orcid.org/0000–0003–2011–1923

REFERENCES

1. Lundberg Båve A, Bergquist A, Bottai M, Warnqvist A, von Seth E, Nordenvall C. Increased risk of cancer in patients with primary sclerosing cholangitis. Hepatol Int. 2021;15:1174–82.
2. Weismüller TJ, Trivedi PJ, Bergquist A, Imam M, Lenzen H, Ponsioen CY, et al. Patient age, sex, and inflammatory bowel disease phenotype associate with course of primary sclerosing cholangitis. Gastroenterology. 2017;152:1975–984.e1978.
3. Ilyas SI, Eaton JE, Gores GJ. Primary sclerosing cholangitis as a premalignant biliary tract disease: Surveillance and management. Clin Gastroenterol Hepatol. 2015;13:2152–65.
4. Karlsen TH, Folseraas T, Thorburn D, Vesterhus M. Primary sclerosing cholangitis—A comprehensive review. J Hepatol. 2017;67:1298–323.
5. Song J, Li Y, Bowlus CL, Yang G, Leung PSC, Gershwin ME. Cholangiocarcinoma in patients with primary sclerosing cholangitis (PSC): A comprehensive review. Clin Rev Allergy Immunol. 2020;58:134–49.
6. Chung BK, Karlsen TH, Folseraas T. Cholangiocytes in the pathogenesis of primary sclerosing cholangitis and development of cholangiocarcinoma. Biochim Biophys Acta Mol Basis Dis. 2018;1864(4 pt B):1390–400.
7. Goeppert B, Folseraas T, Roessler S, Kloor M, Volckmar AL, Endris V, et al. Genomic characterization of cholangiocarcinoma in primary sclerosing cholangitis reveals therapeutic opportunities. Hepatology (Baltimore, Md). 2020;72:1253–66.
8. Kamp EJ, Dinjens WN, Doukas M, van Marion R, Verheij J, Ponsioen CY, et al. Genetic alterations during the neoplastic cascade towards cholangiocarcinoma in primary sclerosing cholangitis. J Pathol. 2022;258:227–35.
9. Holzapfel N, Zhang A, Choi WJ, Denroche R, Jang G, Dodd A, et al. Whole-genome sequencing of 20 cholangiocarcinoma cases reveals unique profiles in patients with cirrhosis and primary sclerosing cholangitis. J Gastrointest Oncol. 2023;14:379–89.
10. Lai Z, Markovets A, Ahdesmaki M, Chapman B, Hofmann O, McEwen R, et al. VarDict: A novel and versatile variant caller for next-generation sequencing in cancer research. Nucleic Acids Res. 2016;44:e108.
11. Forster M, Forster P, Elsharawy A, Hemmrich G, Kreck B, Wittig M, et al. From next-generation sequencing alignments to accurate comparison and validation of single-nucleotide variants: The pibase software. Nucleic Acids Res. 2013;41:e16.
12. Wang K, Li M, Hakonarson H. ANNOVAR: Functional annotation of genetic variants from high-throughput sequencing data. Nucleic Acids Res. 2010;38:e164.
13. Gudmundsson S, Karczewski KJ, Francioli LC, Tiao G, Cummings BB, Alföldi J, et al. Addendum: The mutational constraint spectrum quantified from variation in 141,456 humans. Nature. 2021;597:E3–4.
14. Thorvaldsdottir H, Robinson JT, Mesirov JP. Integrative Genomics Viewer (IGV): High-performance genomics data visualization and exploration. Brief Bioinform. 2013;14:178–92.
15. Sanchez-Vega F, Mina M, Armenia J, Chatila WK, Luna A, La KC, et al. Oncogenic signaling pathways in the Cancer Genome Atlas. Cell. 2018;173:321–37.e310.
16. van Dam TJP, Kennedy J, van der Lee R, de Vrieze E, Wunderlich KA, Rix S, et al. CiliaCarta: An integrated and validated compendium of ciliary genes. PLoS One. 2019;14:e0216705.
17. Vasquez SSV, van Dam J, Wheway G. An updated SYSCILIA gold standard (SCGSv2) of known ciliary genes, revealing the vast progress that has been made in the cilia research field. Mol Biol Cell. 2021;32:br13.
18. Szklarczyk D, Kirsch R, Koutrouli M, Nastou K, Mehryary F, Hachilif R, et al. The STRING database in 2023: Protein-protein association networks and functional enrichment analyses for any sequenced genome of interest. Nucleic Acids Res. 2023;51(D1):D638–d646.
19. Institute B. TARGET Database v32015. Accessed April 14, 2023. https://software.broadinstitute.org/cancer/cga/target.
20. My Cancer Genome. 2011. Accessed December 15, 2022. https://www.mycancergenome.org/.
21. Wardell CP, Fujita M, Yamada T, Simbolo M, Fassan M, Karlic R, et al. Genomic characterization of biliary tract cancers identifies driver genes and predisposing mutations. J Hepatol. 2018;68:959–69.
22. Jusakul A, Cutcutache I, Yong CH, Lim JQ, Huang MN, Padmanabhan N, et al. Whole-genome and epigenomic landscapes of etiologically distinct subtypes of cholangiocarcinoma. Cancer Discov. 2017;7:1116–35.
23. Martínez-Jiménez F, Muiños F, Sentís I, Deu-Pons J, Reyes-Salazar I, Arnedo-Pac C, et al. A compendium of mutational cancer driver genes. Nat Rev Cancer. 2020;20:555–72.
24. Giannakis M, Hodis E, Jasmine Mu X, Yamauchi M, Rosenbluh J, Cibulskis K, et al. RNF43 is frequently mutated in colorectal and endometrial cancers. Nat Genet. 2014;46:1264–6.
25. Kim SJ, Akita M, Sung YN, Fujikura K, Lee JH, Hwang S, et al. MDM2 amplification in intrahepatic cholangiocarcinomas: Its relationship with large-duct type morphology and uncommon KRAS mutations. Am J Surg Pathol. 2018;42:512–21.
26. Yeang CH, McCormick F, Levine A. Combinatorial patterns of somatic gene mutations in cancer. FASEB J. 2008;22:2605–22.
27. Qi X, Li X. Mechanistic insights into the generation and transduction of hedgehog signaling. Trends Biochem Sci. 2020;45:397–410.
28. Loesch R, Chenane L, Colnot S. ARID2 chromatin remodeler in hepatocellular carcinoma. Cells. 2020;9:2152.
29. Fu X, Zhang H, Chen Z, Yang Z, Shi D, Liu T, et al. TFAP2B overexpression contributes to tumor growth and progression of thyroid cancer through the COX-2 signaling pathway. Cell Death Dis. 2019;10:397.
30. Dankner M. Targeted therapy for colorectal cancers with non-V600 BRAF mutations: Perspectives for precision oncology. JCO Precis Oncol. 2018;2:1–12.
31. Harding JJ, Piha-Paul SA, Shah RH, Murphy JJ, Cleary JM, Shapiro GI, et al. Antitumour activity of neratinib in patients with HER2-mutant advanced biliary tract cancers. Nat Commun. 2023;14:630.
32. Goeppert B, Roessler S, Renner M, Singer S, Mehrabi A, Vogel MN, et al. Mismatch repair deficiency is a rare but putative

therapeutically relevant finding in non-liver fluke associated cholangiocarcinoma. Br J Cancer. 2019;120:109–14.
33. Guo P, Pu T, Chen S, Qiu Y, Zhong X, Zheng H, et al. Breast cancers with EGFR and HER2 co-amplification favor distant metastasis and poor clinical outcome. Oncol Lett. 2017;14:6562–70.
34. Grigoriev I, Yu KL, Martinez-Sanchez E, Serra-Marques A, Smal I, Meijering E, et al. Rab6, Rab8, and MICAL3 cooperate in controlling docking and fusion of exocytotic carriers. Curr Biol: CB. 2011;21:967–74.
35. Bachmann-Gagescu R, Dona M, Hetterschijt L, Tonnaer E, Peters T, de Vrieze E, et al. The ciliopathy protein CC2D2A associates with NINL and functions in RAB8-MICAL3-regulated vesicle trafficking. PLoS Genet. 2015;11:e1005575.
36. Cullinane AR, Schäffer AA, Huizing M. The BEACH is hot: A LYST of emerging roles for BEACH-domain containing proteins in human disease. Traffic. 2013;14:749–66.
37. Langbein L, Rogers MA, Praetzel-Wunder S, Helmke B, Schirmacher P, Schweizer J. K25 (K25irs1), K26 (K25irs2), K27 (K25irs3), and K28 (K25irs4) represent the type I inner root sheath keratins of the human hair follicle. J Invest Dermatol. 2006;126:2377–86.
38. Bond GL, Hu W, Bond EE, Robins H, Lutzker SG, Arva NC, et al. A single nucleotide polymorphism in the MDM2 promoter attenuates the p53 tumor suppressor pathway and accelerates tumor formation in humans. Cell. 2004;119:591–602.
39. Yarlagadda B, Kamatham V, Ritter A, Shahjehan F, Kasi PM. Trastuzumab and pertuzumab in circulating tumor DNA ERBB2-amplified HER2-positive refractory cholangiocarcinoma. NPJ Precis Oncol. 2019;3:19.
40. Kacew A, Sweis RF. FGFR3 alterations in the era of immunotherapy for urothelial bladder cancer. Front Immunol. 2020;11:575258.
41. Boehringer I Brightline-2: A study to test whether BI 907828 helps people with cancer in the biliary tract, pancreas, lung or bladder. 2025. Accessed March 20, 2023. https://ClinicalTrials.gov/show/NCT05512377.
42. Przybyl J, van de Rijn M, Rutkowski P. Detection of SS18-SSX1/2 fusion transcripts in circulating tumor cells of patients with synovial sarcoma. Diagn Pathol. 2019;14:24.
43. Yong LK, Lai S, Liang Z, Poteet E, Chen F, van Buren G, et al. Overexpression of Semaphorin-3E enhances pancreatic cancer cell growth and associates with poor patient survival. Oncotarget. 2016;7:87431–48.
44. Mayr C, Kiesslich T, Modest DP, Stintzing S, Ocker M, Neureiter D. Chemoresistance and resistance to targeted therapies in biliary tract cancer: What have we learned? Expert Opin Investig Drugs. 2022;31:221–33.
45. Hallin J, Bowcut V, Calinisan A, Briere DM, Hargis L, Engstrom LD, et al. Anti-tumor efficacy of a potent and selective non-covalent KRAS(G12D) inhibitor. Nat Med. 2022;28:2171–82.
46. Ciombor KK, Strickler JH, Bekaii-Saab TS, Yaeger R. BRAF-mutated advanced colorectal cancer: A rapidly changing therapeutic landscape. J Clin Oncol. 2022;40:2706–15.
47. Kendall T, Verheij J, Gaudio E, Evert M, Guido M, Goeppert B, et al. Anatomical, histomorphological and molecular classification of cholangiocarcinoma. Liver Int. 2019;39(suppl 1):7–18.
48. Kinzler MN, Schulze F, Bankov K, Gretser S, Becker N, Leichner R, et al. Impact of small duct- and large duct type on survival in patients with intrahepatic cholangiocarcinoma: Results from a German tertiary center. Pathol Res Pract. 2022;238:154126.
49. Mansini AP, Peixoto E, Thelen KM, Gaspari C, Jin S, Gradilone SA. The cholangiocyte primary cilium in health and disease. Biochim Biophys Acta Mol Basis Dis. 2018;1864(4 Pt B):1245–53.
50. Pant K, Richard S, Gradilone SA. Short-chain fatty acid butyrate induces cilia formation and potentiates the effects of HDAC6 inhibitors in cholangiocarcinoma cells. Front Cell Dev Biol. 2021;9:809382.

How to cite this article: Grimsrud MM, Forster M, Goeppert B, Hemmrich-Stanisak G, Sax I, Grzyb K, et al. Whole-exome sequencing reveals novel cancer genes and actionable targets in biliary tract cancers in primary sclerosing cholangitis. Hepatol Commun. 2024;8:e0461. https://doi.org/10.1097/HC9.0000000000000461